Available online at www.sciencedirect.com

ScienceDirect

Mendeleev Commun., 2022, **32**, 810–812

Mendeleev Communications

Osteoconductive biocompatible 3D-printed composites of poly-D,L-lactide filled with nanocrystalline cellulose modified by poly(glutamic acid)

Ilia V. Averianov,[a] Mariia A. Stepanova,[a] Iosif V. Gofman,[a] Antonina Lavrentieva,[b] Viktor A. Korzhikov-Vlakh[c] and Evgenia G. Korzhikova-Vlakh*[a,c]

[a] *Institute of Macromolecular Compounds, Russian Academy of Sciences, 199004 St. Petersburg, Russian Federation. E-mail: vlakh@hq.macro.ru*
[b] *Institute of Technical Chemistry, Leibniz Universität Hannover, 30167 Hannover, Germany*
[c] *Institute of Chemistry, St. Petersburg State University, 198504 St. Petersburg, Russian Federation*

DOI: 10.1016/j.mencom.2022.11.034

Three dimensional composite matrices based on poly-D,L-lactide filled with 5 or 10 wt% of nanocrystalline cellulose modified by poly(glutamic acid) were produced using pre-optimized 3D printing technique. The composites demonstrated good biocompatibility and significantly improved osteoconductive properties compared with the matrix without filler or the one filled with neat nanocrystalline cellulose.

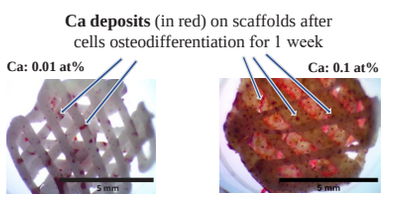

Keywords: poly-D,L-lactide, modified nanocrystalline cellulose, poly(glutamic acid), composite three dimensional matrix, 3D printing, osteoconductive material, biomineralization, bone regeneration.

Scaffolds represent three dimensional (3D) artificial biocompatible and biodegradable materials that support cell growth and osteodifferentiation to control and accelerate the regeneration of bone defects with a critical size. Their development is of great interest for advanced bioengineering and materials science.[1–5] 3D printing with fused deposition modeling represents an advanced technology for manufacturing of the scaffolds with dedicated architecture to ensure a successful implant integration and bone repair.[1,2,6–10] Biodegradable aliphatic polyesters[11–13] like polylactide (PLA), poly(lactide-*co*-glycolide) (PLGA) and poly(ε-caprolactone) (PCL) constitute the key polymers for preparation of the scaffolds by 3D printing.[11,14–19] Their hydrophobicity and absence of biological activity[14,20] are typically adjusted by inclusion of inorganic or organic stimulating and signaling substances or particles to provide attachment and viability of osteoblasts followed by the formation of bone tissue (*i.e.*, osteoconductivity) as well as to increase Ca-containing mineral deposits.[1,21–24] Cellulose micro- and nanomaterials are employed as promising fillers for these key polymers due to biocompatibility, high hydrophilicity, ability to cell adhesion and proliferation, low cost, the presence of reactive groups for modification as well as suitable mechanical properties.[2,3,25,26] Addition of micro- or nanocrystalline cellulose (NCC) to aliphatic polyesters allows one to adjust the mechanical properties and degradation rate of the composite as well as ensure the desired spatial and temporal distribution of the stimulating/signaling molecules in the final matrix.[2,25] The effect was demonstrated[27] for a glutamic acid-rich peptide attached to the surface of PLA/PLGA nanofibers on the formation of calcium phosphate crystals and thereby an increase in the osteogenic differentiation of marrow stromal cells.

Our group reported an approach to modification of NCC by poly(glutamic acid) (polyGlu)[28] and application of the material as a filler for composite films based on poly-L-lactide (PLLA), poly-D,L-lactide (PDLLA) and PCL.[20,28,29] The composites with polyGlu-modified NCC had improved tensile properties,[20] revealed good biocompatibility *in vivo*[20] and contributed to the formation of Ca deposits in cell free media.[20,29] Given the scaffold architecture, which depends on pore size, morphology and interpermeability, represents a key factor for cells attachment and viability,[2,6,7,30] the purpose of this work was to develop 3D-printed composite scaffolds based on PDLLA and NCC–polyGlu as well as evaluate their mechanical and osteoconductive properties.

The synthesis and characterization of polyGlu were performed† as described in our works.[28,31] The weight-average molecular weight (M_w) and dispersity ($Đ$) from SEC as well as the amount of residual benzyl protecting groups from ^{1}H NMR for the obtained polymer were 2100, 1.05 and 22%, respectively. The incompletely removed benzyl groups imparted amphiphilic properties to the polyGlu chains to improve the integration of filler particles modified by them into the polymer matrix. Modification of NCC with polyGlu was carried out *via* periodate oxidation, imine bonds formation and their subsequent reduction with sodium borohydride as described.[20,28] PDLLA with M_w = 169,000 and $Đ$ = 1.9 (from SEC) was obtained using the known conditions.[20] Nonporous composite materials based on PDLLA and 5 or 10 wt% unmodified NCC, designated as PDLLA/NCC(5) or PDLLA/NCC(10), respectively, as well as modified NCC [PDLLA/NCC–polyGlu(5) and PDLLA/NCC–polyGlu(10)] as fillers were prepared by melt blending. The following mechanical characteristics for compression of the obtained samples were determined: Young's modulus (E), the force applied at maximum compression (F_{max}), plasticity limit (σ_p) and compressive strength (σ_{max}). For details of the

† PolyGlu was prepared by ring-opening polymerization of *N*-carboxyanhydride of γ-*O*-benzyl-α-glutamic acid with following deprotection using trifluoromethanesulfonic acid in TFA. The product was analyzed by SEC and ^{1}H NMR.

Table 1 Mechanical characteristics for nonporous PDLLA and its composite materials determined by a compression test.

Material	*E*/GPa	F_{max}/kN	σ_p/MPa	σ_{max}/MPa
PDLLA	2.02 ± 0.12	38.57 ± 0.93	103 ± 2	341 ± 5
PDLLA/NCC(5)	1.47 ± 0.09	40.67 ± 0.81	107 ± 2	360 ± 7
PDLLA/NCC(10)	1.43 ± 0.11	37.21 ± 0.56	93 ± 1	329 ± 10
PDLLA/NCC–polyGlu(5)	1.71 ± 0.12	40.60 ± 0.53	94 ± 2	359 ± 9
PDLLA/NCC–polyGlu(10)	1.53 ± 0.08	33.93 ± 0.37	79 ± 1	300 ± 6

preparation and testing, see Online Supplementary Materials. The results are presented in Table 1 and Figure S1.

All the tested materials demonstrated a plastic deformation with high resource, namely, none of the samples fractured under compression up to 70%. The mechanical parameters determined for all the composites were close to the ones for pristine PDLLA or slightly exceeded them, with the exception of Young's modulus, which was lower for all the composites probably due to inhomogeneous areas resulted from the filler aggregation. However, slightly higher values of Young's modulus were observed for PDLLA/NCC–polyGlu compared with PDLLA/NCC with a similar amount of the filler, which indicated greater interfacial compatibility between PDLLA and NCC–polyGlu. This assumption was also confirmed by our investigations of tensile mechanical properties for films based on aliphatic polyesters and NCC as well as NCC modified with polyGlu or polylactide, where a significant improvement in mechanical properties due to the modifications had been observed.[20,28,29,32] Thus, all the composites obtained here were characterized by acceptable mechanical properties, despite some reduction in mechanical values for compression relative to pristine PDLLA.

To produce 3D-printed composite scaffolds, the printing parameters were initially adjusted using pure PDLLA. For optimization of the matrix architecture, it is necessary to take into account that the size of pores and their interpermeability play a crucial role in the bone formation *in vivo*. The use of scaffolds with a pore size of 20–1500 μm for filling bone defects has been widely discussed.[1,11,13] In particular, it is known that mineralized bone tissue and vascularization can be achieved when the scaffolds with a pore size from 200 and 300 μm, respectively, are used. At the same time, the proper cell reproduction occurs with pores ⩽ 1000 μm. Thus, to ensure the mutual permeability of the material pores, the optimal printing parameters for PDLLA multilayer products were determined (for details of printing options with step-by-step graphical support, see Online Supplementary Materials).‡ Figure 1(*a*)–(*c*) demonstrates a photo and SEM images§ of an example of 3D-printed PDLLA-based matrix with a smooth and uniform structure of the material.

Using the optimized conditions, the composite 3D matrices of a similar structure were printed. Samples with a diameter of 7–9 mm, a height of ~1 mm and a pore size of ~1000 μm consisted of three layers and contained 5 or 10 wt% NCC or NCC–polyGlu. Morphology of the composites slightly differed from the one for the PDLLA samples [Figure 1(*d*)–(*g*)] and was characterized by more pronounced roughness with higher amount of the filler. However, for PDLLA/NCC–polyGlu a much smaller number and size of filler aggregates as well as surface irregularities were observed, which indicated better

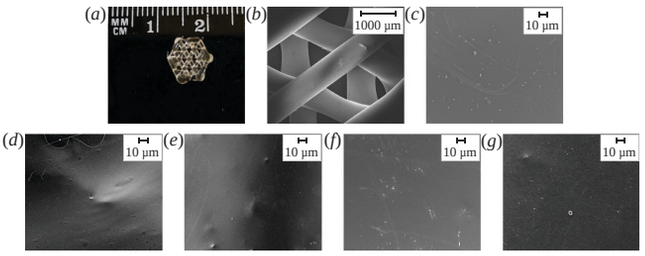

Figure 1 (*a*) Photo and (*b*)–(*g*) SEM images of 3D-printed PDLLA and its composites: (*a*)–(*c*) PDLLA, (*d*) PDLLA/NCC(5), (*e*) PDLLA/NCC(10), (*f*) PDLLA/NCC–polyGlu(5) and (*g*) PDLLA/NCC–polyGlu(10).

compatibility of the matrix and the partially deblocked polyGlu-modified NCC filler.

Since the acceptable mechanical properties and homogeneous morphology had been observed for composites containing both 5 and 10 wt% of the filler, the 3D-printed composites containing 10 wt% of the NCC or NCC–polyGlu filler were selected for further investigation of their osteoconductive properties. This choice was also motivated by the assumption that higher filler content and hence more polyGlu residues would promote intensive formation of Ca-containing mineral deposits, *i.e.*, mineralization, for rather rapidly degrading PDLLA. An *in vitro* biomineralization was explored using human adipose derived mesenchymal stem cells (hMSCs). After cell adhesion and further proliferation, the scaffolds were placed in an osteogenic medium for osteodifferentiation (for detailed conditions of sterilization, cultivation and differentiation, see Online Supplementary Materials).¶ SEM images of the materials before and after the procedures clearly demonstrate significant changes in their surface probably caused by cell adhesion and proliferation as well as the formation of Ca deposits (Figure S3).

A drastic increase in Ca deposits for PDLLA/NCC–polyGlu scaffolds after the osteodifferentiation and the extremely scarce ones for other materials were evidenced using alizarin red S as a Ca-specific dye (Figure 2)†† and by energy dispersive X-ray analysis (EDX). According to both methods, the highest relative content of Ca was observed for the PDLLA/NCC–polyGlu(10) scaffold. This result could not be associated with an increase in the number of hMSCs adhered at the surface after incubation in the growth medium, which was confirmed by the standard CellTiter-Blue cell viability assay (Figure S4). Thus, the deposits formed represented a result of osteodifferentiation. For more data from the EDX analysis for PDLLA/NCC–polyGlu(10) before and after the osteogenic differentiation, see Online Supplementary Materials, including Figures S5 and S6.

Thus, the use of polyGlu-modified NCC as a filler for PDLLA definitely contributed to improved osteoconductive properties of the developed 3D-printed composites *in vitro*. The tendency in the formation of Ca deposits appeared to be similar to our results in the mineralization study of the same composites as films using their alternate incubation in a cell-free medium with Ca^{2+} and $H_2PO_4^-$ for 30 weeks. The amount of Ca deposits there increased significantly for NCC–polyGlu as a filler. Moreover, elevation of the filler content from 5 to 15 wt% also improved the mineralization.[20]

In summary, 3D printing conditions were developed and homogeneous PDLLA-based scaffolds using pure and polyGlu-

‡ Modeling and printing of samples was carried out using a GeSiM 3D printer (Germany) with pneumatic extruder and the proprietary software.
§ SEM images were acquired using a Zeiss Auriga microscope (Germany).

¶ After sterilization, each matrix was seeded with hMSCs. Cells were cultivated in a growth medium for 2 weeks, then their osteogenic differentiation was carried out in a dedicated medium for 1 week.
†† The matrices were fixed in 4% aqueous solution of paraformaldehyde and stained with alizarin red S dye to visualize Ca deposits. Images of the stained samples were recorded using a Nikon Eclipse E200 optical microscope (Japan) with an U3CMOS digital camera and the NIS-Elements software.

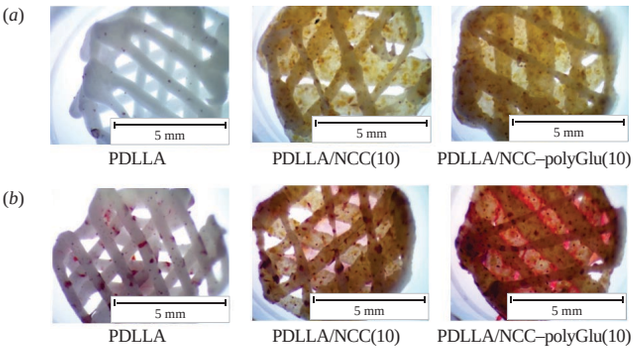

Figure 2 PDLLA and its composite scaffolds stained by alizarin red S dye: (*a*) after procedure in the growth medium, (*b*) after procedure in the osteogenic differentiation medium. The intensity of red color appeared after staining is proportional to the mineral deposits on the scaffold surface.

modified NCC as a filler were obtained. Despite the hydrophilic properties of the filler, the mechanical properties of PDLLA-based composites were retained at a level close to neat PDLLA. The best mechanical properties were determined for the composites with 5 wt% of the filler. Further investigation of the osteoconductive properties of 3D-printed PDLLA/NCC–polyGlu composites *in vitro* demonstrated their good biocompatibility as well as a significant increase in mineralization due to improved osteodifferentiation of cells induced by the presence of polyGlu. The developed composites seem to be promising scaffolds for bone tissue regeneration.

SEM and EDX analyses were performed using the equipment of the Interdisciplinary Center for Nanotechnology of the St. Petersburg State University Research Park (megagrant no. 075-15-2021-637).

Online Supplementary Materials

Supplementary data associated with this article can be found in the online version at doi: 10.1016/j.mencom.2022.11.034.

References

1 C. Fernandes, C. Moura, R. M. T. Ascenso, S. Amado, N. Alves and P. Pascoal-Faria, in *Design and Manufacturing*, eds. E. Yasa, M. Mhadhbi and E. Santecchia, IntechOpen, 2020, pp. 161–186.
2 X. Zhang, X. Yin, J. Luo, X. Zheng, H. Wang, J. Wang, Z. Xi, X. Liao, J. O. Machuki, K. Guo and F. Gao, *ACS Biomater. Sci. Eng.*, 2019, **5**, 294.
3 M. Ansari, *Prog. Biomater.*, 2019, **8**, 223.
4 L. M. Witting, A.-C. Waselau, F. Feichtner, L. Wurm, S. Julmi, C. Klose, A.-K. Gartzke, H. J. Maier, P. Wriggers and A. Meyer-Lindenberg, *Materialia*, 2020, **14**, 100949.
5 R. Dimitriou, E. Jones, D. McGonagle and P. V. Giannoudis, *BMC Med.*, 2011, **9**, 66.
6 D. P. Bhattarai, M. H. Kim, H. Park, W. H. Park, B. S. Kim and C. S. Kim, *Chem. Eng. J.*, 2020, **389**, 123470.
7 H. Eftekhari, A. Jahandideh, A. Asghari, A. Akbarzadeh and S. Hesaraki, *Artif. Cells, Nanomed., Biotechnol.*, 2017, **45**, 961.
8 L. Roseti, V. Parisi, M. Petretta, C. Cavallo, G. Desando, I. Bartolotti and B. Grigolo, *Mater. Sci. Eng., C*, 2017, **78**, 1246.
9 M. Stepanova, A. Eremin, I. Averianov, I. Gofman, A. Lavrentieva, V. Korzhikov-Vlakh and E. Korzhikova-Vlakh, *Key Eng. Mater.*, 2019, **822**, 277.
10 E. G. Gordeev and V. P. Ananikov, *Russ. Chem. Rev.*, 2020, **89**, 1507.
11 R. Donate, M. Monzón and M. E. Alemán-Domínguez, *e-Polym.*, 2020, **20**, 571.
12 K. Hara, E. Hellem, S. Yamada, K. Sariibrahimoglu, A. Mølster, N. R. Gjerdet, S. Hellem, K. Mustafa and M. A. Yassin, *Mater. Today Bio*, 2022, **14**, 100237.
13 J. Henkel, M. A. Woodruff, D. R. Epari, R. Steck, V. Glatt, I. C. Dickinson, P. F. M. Choong, M. A. Schuetz and D. W. Hutmacher, *Bone Res.*, 2013, **1**, 216.
14 Z. Fu, J. Cui, B. Zhao, S. G. Shen and K. Lin, *J. Orthop. Transl.*, 2021, **28**, 118.
15 A. J. R. Lasprilla, G. A. R. Martinez, B. H. Lunelli, A. L. Jardini and R. M. Filho, *Biotechnol. Adv.*, 2012, **30**, 321.
16 K. Budak, O. Sogut and U. A. Sezer, *J. Polym. Res.*, 2020, **27**, 208.
17 M. A. Woodruff and D. W. Hutmacher, *Prog. Polym. Sci.*, 2010, **35**, 1217.
18 R. Dwivedi, S. Kumar, R. Pandey, A. Mahajan, D. Nandana, D. S. Katti and D. Mehrotra, *J. Oral Biol. Craniofacial Res.*, 2020, **10**, 381.
19 Yu. V. Ermolenko, A. S. Semyonkin, Yu. V. Ulianova, T. S. Kovshova, O. O. Maksimenko and S. E. Gelperina, *Russ. Chem. Bull.*, 2020, **69**, 1416.
20 M. Stepanova, I. Averianov, M. Serdobintsev, I. Gofman, N. Blum, N. Semenova, Y. Nashchekina, T. Vinogradova, V. Korzhikov-Vlakh, M. Karttunen and E. Korzhikova-Vlakh, *Materials*, 2019, **12**, 3435.
21 K. A. Blackwood, N. Bock, T. R. Dargaville and M. A. Woodruff, *Int. J. Polym. Sci.*, 2012, 174942.
22 M. Tallawi, E. Rosellini, N. Barbani, M. G. Cascone, R. Rai, G. Saint-Pierre and A. R. Boccaccini, *J. R. Soc., Interface*, 2015, **12**, 20150254.
23 M. Stepanova, O. Solomakha, M. Rabchinskii, I. Averianov, I. Gofman, Y. Nashchekina, G. Antonov, A. Smirnov, B. Ber, A. Nashchekin and E. Korzhikova-Vlakh, *Polymers*, 2021, **13**, 2628.
24 I. I. Preobrazhensky, A. A. Tikhonov, E. S. Klimashina, P. V. Evdokimov and V. I. Putlyaev, *Russ. Chem. Bull.*, 2020, **69**, 1601.
25 M. Stepanova and E. Korzhikova-Vlakh, *Polymers*, 2022, **14**, 1477.
26 X. Zhang, C. Wang, M. Liao, L. Dai, Y. Tang, H. Zhang, P. Coates, F. Sefat, L. Zheng, J. Song, Z. Zheng, D. Zhao, M. Yang, W. Zhang and P. Ji, *Carbohydr. Polym.*, 2019, **213**, 27.
27 O. Karaman, A. Kumar, S. Moeinzadeh, X. He, T. Cui and E. Jabbari, *J. Tissue Eng. Regener. Med.*, 2016, **10**, E132.
28 I. V. Averianov, M. A. Stepanova, I. V. Gofman, A. L. Nikolaeva, V. A. Korzhikov-Vlakh, M. Karttunen and E. G. Korzhikova-Vlakh, *Mendeleev Commun.*, 2019, **29**, 220.
29 M. Stepanova, I. Averianov, O. Solomakha, N. Zabolotnykh, I. Gofman, M. Serdobintsev, T. Vinogradova, V. Korzhikov-Vlakh and E. Korzhikova-Vlakh, *J. Renewable Mater.*, 2020, **8**, 383.
30 A. A. Gutsalova, D. A. Fedorishin, D. N. Lytkina and I. A. Kurzina, *Mendeleev Commun.*, 2021, **31**, 382.
31 A. A. Vdovchenko, A. V. Hubina, E. G. Vlakh and T. B. Tennikova, *Mendeleev Commun.*, 2017, **27**, 153.
32 M. Stepanova, I. Averianov, I. Gofman, O. Solomakha, Y. Nashchekina, V. Korzhikov-Vlakh and E. Korzhikova-Vlakh, *IOP Conf. Ser.: Mater. Sci. Eng.*, 2019, **500**, 012021.

Received: 25th April 2022; Com. 22/6879